Geophys. J. Int. (2006) **164,** 290–300 doi: 10.1111/j.1365-246X.2005.02820.x

Anomalously shallow inclination in middle–northern part of the South China block: palaeomagnetic study of Late Cretaceous red beds from Yichang area

Kazutoshi Narumoto,[1] Zhenyu Yang,[2] Kazuhiro Takemoto,[1] Haider Zaman,[1] Hayao Morinaga[3] and Yo-ichiro Otofuji[1]

[1]*Department of Earth and Planetary Sciences, Faculty of Science, Kobe University, Kobe* 675-8501, *Japan. E-mail: otofuji@kobe-u.ac.jp*
[2]*Department of Earth Sciences, Nanjing University, Nanjing, China*
[3]*Department of Global Tectonics, Graduate School of Life Sciences, University of Hyogo, Shosha* 2167, *Himeji* 671-2201, *Japan*

Accepted 2005 September 27. Received 2005 September 24; in original form 2005 March 7

SUMMARY

We present new palaeomagnetic results from Late Cretaceous red beds of the Paomagang Formation collected at 42 sites in the Yichang area (30.7°N, 111.7°E), middle–northern part of the South China Block. A high unblocking temperature component around 680°C was isolated from 26 sites by stepwise thermal demagnetization. Fold tests are positive at the 95 per cent confidence limit for 14 and 11 sites of the Paomagang and Wangdian areas, respectively. Normal and reversed polarity sequence found in the Wangdian area passed a reversal test at the 95 per cent confidence limit. The tilt-corrected mean direction for Yichang area is $D = 3.8°$, $I = 23.3°$ ($\alpha_{95} = 5.1°$, $N = 26$), corresponding to a palaeopole at 71.5°N, 280.0°E with $A_{95} = 4.3°$. Comparison with the expected inclination from the 80 Ma Eurasian APWP pole indicates a inclination flattening of 26.3° ± 6.4°. Middle Cretaceous to Cenozoic NW–SE extension tectonics within the SCB contributes only 2.0° to the inclination flattening. While the massive samples of the Paomagang Formation show a moderate degree of anisotropy ($1.017 < Pj < 1.086$) and steeper inclination ($I = 29.3°$), the laminated samples, which form more than 75 per cent of the studied samples, show a higher degree of anisotropy ($1.052 < Pj < 1.227$) and shallower inclination value ($I = 22.7°$). A good correlation between remanence inclination and facies types indicates that depositional processes produced the observed shallow inclination in the Yichang area.

Key words: Cretaceous, depositional process, inclination shallowing, palaeomagnetism, SCB, tectonics.

1 INTRODUCTION

Anomalously low inclinations in palaeomagnetic directions have been reported from Cretaceous to Palaeogene rocks of the Asian continent (Cogne *et al.* 1999; Chauvin *et al.* 1996; Bazhenov & Mikolaichuk 2002), since Westphal *et al.* (1986) noticed the low palaeolatitude in the Tethyan mobile belt at Eocene and Oligocene times. The low palaeomagnetic inclination in these regions has been explained in three different ways; variation in the nature of the geomagnetic field (Westphal *et al.* 1986; Chauvin *et al.* 1996), large-scale tectonic motions (e.g. Chen *et al.* 2002) and sedimentological mechanisms that resulted in inclination flattening (Gilder *et al.* 2001; Bazhenov & Mikolaichuk 2002; Tan *et al.* 2003).

Post-Eocene northward displacement is invoked for the tectonic blocks in Asia (Tapponnier *et al.* 1982; Houseman & England 1986) because the Indian continent collided with the Asian continent at about 55 Ma. Evidence of northward movement for central and eastern Asia includes the observed anomalously low palaeomagnetic inclinations of Cretaceous to Palaeogene sedimentary rocks in Tarim, Tien Shan, Junggar, northern Tibet and Hexi Corridor (Li *et al.* 1988; Chen *et al.* 1991, 1992, 2002; Thomas *et al.* 1993), however, non-rigid behaviour of the Eurasian continent was proposed as an alternate solution (Cogne *et al.* 1999) to reconcile low inclinations in Palaeogene rocks distributed through central Asia. Because the low inclination of tectonic origin is inevitable in the northward-moving terranes and non-rigid continental blocks, it is hard to discriminate tectonic effects from low inclination origin of rocks in these tectonic blocks (e.g. Chen *et al.* 2002).

Palaeomagnetic studies from the South China Block (SCB) (Yang & Besse 2001; Morinaga & Liu 2004) show that the SCB has been rigid and subjected to no relative displacement with the North China Block (NCB) and Eurasia since Cretaceous times (Morinaga & Liu 2004) (Fig. 1). Therefore, we focused our palaeomagnetic study on the SCB and collected samples from the Yichang area (30.7°N,

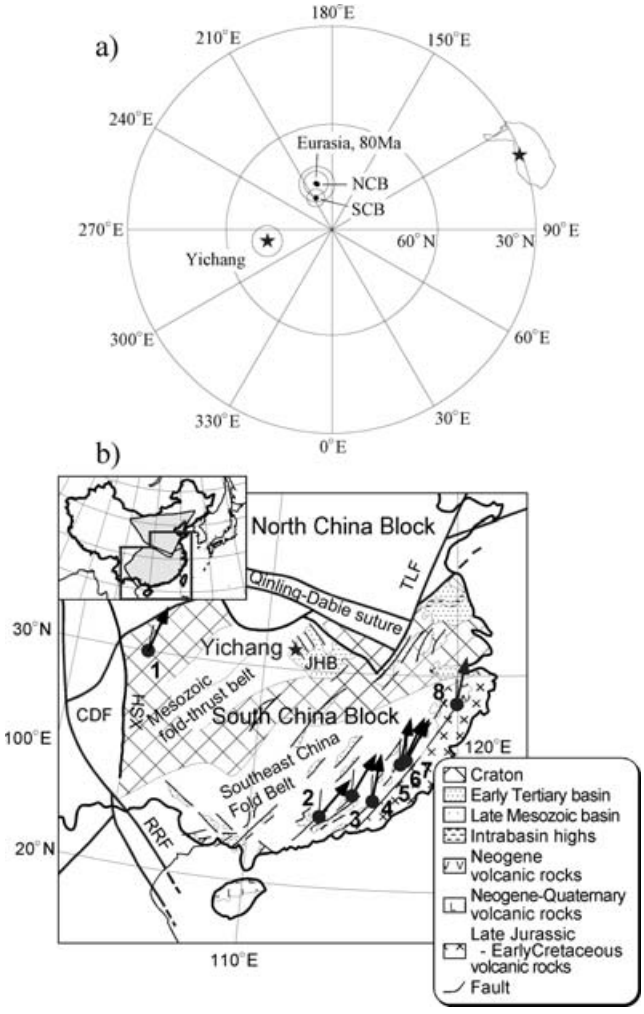

Figure 1. (a) The Late Cretaceous palaeomagnetic pole for the Yichan area compared with those for the NCB, SCB and Eurasia. Late Cretaceous palaeomagnetic pole (with associated circles or ellipse of 95 per cent confidence level) for the Yichang area (71.5°N, 280.0°E, $A_{95} = 4.3°$) is shown by the star, and others shown are by closed circles; the SCB (80.0°N, 206.7°E, $A_{95} = 2.5°$), the NCB (76.5°N, 198.0°E, $A_{95} = 5.0°$) and the Eurasia (80 Ma; 76.2°N, 198.9°E and $A_{95} = 3.4°$). (b) Simplified tectono-geographic sketch map for the South China Block. CDF: Chuan Dian fragment, JHB: Jianghan basin, TLF: Tan-Lu fault, RRF: Red river fault, XSH: Xian Shui He fault. Black arrows indicate declinations in the Late Cretaceous palaeomagnetic declinations by which Morinaga & Liu (2004) calculate the mean palaeomangetic pole for the SCB; 1. Feixianguan/Xinjin/Guanyin, 2. Guangzhou, 3. No Guangdong, 4. Guangdong Province, 5. Fujian Province, 6. Yongan, 7. Yong'an, and 8. Zhejiang Province (Enkin *et al.* 1991a; Gilder *et al.* 1993; Morinaga & Liu 2004).

111.7°E) of its middle–northern part (Fig. 1b). No palaeomagnetic data have been published from this area because of the paucity of sedimentary strata suitable for fold test. This is probably due to stable platform nature of the SCB where the sedimentary strata maintain nearly horizontal attitude (Li 1998).

2 GEOLOGICAL SETTING OF THE YICHANG AREA AND PALAEOMAGENTIC SAMPLING

The Late Cretaceous to Tertiary sedimentary strata is sporadically distributed along the northwestern margin of the Jianghan Basin (JHB), northeastern part of the Mesozoic fold-thrust belt (Figs 1 and 2). These Late Cretaceous strata consist of red sandstones of the Shimen, Wulong, Luojingtan, Honghuatao and Paomagang Formations in ascending order. Late Cretaceous age for the Paomagang Formation is well constrained by the presence of diatom (*Porochara–Latochara–Obtusochara*) and bivalve (*Talicypridea–Cypridea–Clinocypris*) assemblages, together with fossils of *Macroolithus yaotunensis* and *Knightia yuyanga* (BGMRHN 1988). The Tertiary Gongjiachong Formatioin conformably overlies the Paomagang Formation.

Gentle folding is observed in the Paomagang Formation around the Yichang area, which is located on northeast side of the Mesozoic fold-thrust belt. We collected palaeomagnetic samples from the purplish-red sandstone of this formation. Samples were collected at 42 sites in the Paomagang and Wangdian areas, about 30 km towards east from Yichang (Fig. 2). A total of 136 samples (16 sites) were collected from two localities at South and North Paomagang, where a monoclinal structure is observed (Fig. 2b). Strata at these localities dip nearly southeast from 1° to 16°. From the Wangdian area, we collected 238 samples (26 sites) at three localities, that is, West, East and North Wangdian (Fig. 2a). Dips of strata at the West Wangdian locality vary between 21° and 53° towards the west, and those at the east Wangdian locality vary between 5° and 13° towards the east. Because the stratigraphic relations among the sampling sites are well determined within each locality, sampling sites are arranged in descending order (as listed in Table 1). Unfortunately stratigraphic relationships among the localities are not clear.

Palaeomagnetic samples were collected using a portable core drill and oriented with a magnetic compass. Four to 14 oriented samples were collected over a distance of 10 m at each site. Since each site consists of several layers of strata, at least one sample from each layer was collected. The present geomagnetic field declination value at each sampling site was calculated using the International Geomagnetic Reference Field (Mandea & Macmillan 2000).

3 LABORATORY PROCEDURES

In the laboratory, 2.3-cm-long specimens were prepared from each sample. Natural remanent magnetization (NRM) of each specimen was measured using a cryogenic magnetometer (2G-Enterprises) of the Kobe University Palaeomagnetic Laboratory. All specimens were subjected to stepwise thermal demagnetization using a Natsuhara TDS-1 thermal demagnetizer. The residual field of this demagnetizer was less than 5 nT. On average, 17 heating steps were made up to 690°C. The thermal demagnetization temperature interval was as small as 5°C between 670°C and 690°C. In order to monitor magnetic mineral alteration during progressive heating, bulk magnetic susceptibility of each specimen was measured after each demagnetization step using a Bartington MS2 system. Magnetic behaviour of each specimen after demagnetization was plotted on a Zijderveld diagram (Zijderveld 1967). Principal component analysis (Kirschvink 1980) was used to identify magnetic components. Site mean directions were calculated using Fisherian statistics (Fisher 1953).

Progressive acquisition of isothermal remanent magnetization (IRM) was performed up to a maximum DC field of 2.7T using a 2G pulse magnetizer. Thermal demagnetization of the composite IRMs (Lowrie 1990) was carried out to investigate the unblocking spectra of selected specimens. Several specimens were subjected to strong-field thermomagnetic analysis to identify ferromagnetic

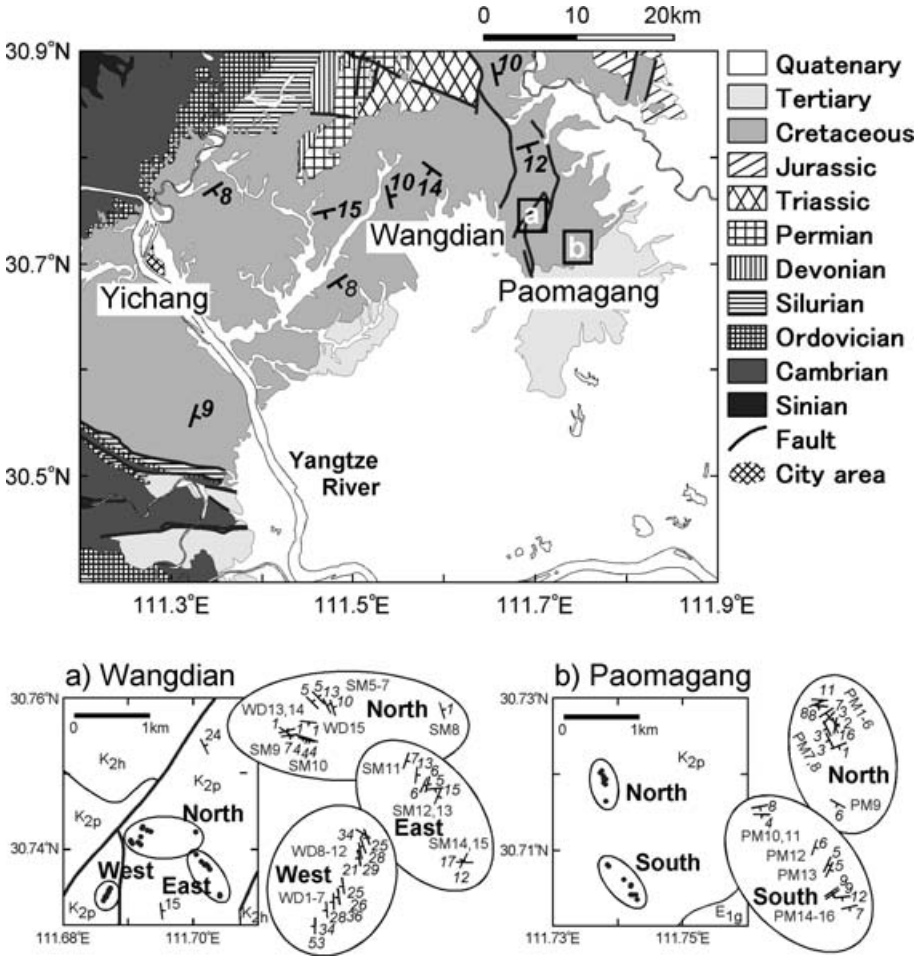

Figure 2. Simplified geological sketch map of the Wangdian and Paomagang areas. Black lines indicate faults. (a) and (b) are sampling localities in the Wangdian and Paomagang areas. Bedding attitudes at each sampling site in five localities (North Wangdian, West Wangdian, East Wangdaian, North Paomagang and South Paomagang) are shown in inset. K2p: Late Cretaceous Paomagang Formation, K2h: Late Cretaceous Honghuatao Formation, E1g: Eocene Gongjiachong Formation.

minerals using an automatic recording thermomagnetic balance at Kyoto University.

Anisotropy of magnetic susceptibility (AMS) studies was carried out on samples from the Paomagang Formation using an AGICO KLY-3S susceptibility bridge at the Faculty of Human Development, Kobe University. AMS data were analysed following the method of Tarling & Hrouda (1993). Principal susceptibilities of $K_{max} \geq K_{int} \geq K_{min}$ were determined. Corrected anisotropy degree (P_j) and shape parameter (T) were calculated. In addition to the Paomagang Formation, we also measured red bed samples of the Shaxian and Chongan formations (Southeast China Fold belt) from which reliable palaeomagnetic data with few inclination flattening values are reported by Morinaga & Liu (2004).

4 ROCK MAGNETIC RESULTS

Strong-field thermomagnetic experiments (Figs 3a and b) for the samples of Paomagang and Wangdian areas suggest a predominance of haematite as the magnetic carrier. Curie temperatures around 685°C are observed, both on heating and cooling. IRM acquisition curves (Figs 3c and d) show that no saturation is achieved up to the maximum field of 2.7T, indicating the dominance of high-coercivity minerals, such as haematite or/and goethite. The presence of haematite is indicated by thermal demagnetization of the composite IRMs, while goethite is not clearly visible in the curves (Figs 3e and f).

The AMS results from Paomagang Formation show a predominantly oblate ellipsoid. Tilt-corrected AMS data for typical specimens show that the minimum axes are nearly perpendicular to bedding, while maximum and intermediate axes are dispersed on a bedding plane (Fig. 4). We interpret these distributions as representative of the sedimentary origin fabric, with no significant tectonically deformation effects. The AMS results show high value in the corrected anisotropy degree (Pj) up to 1.227.

As reported by Garces *et al.* (1996), strong anisotropy dominates in the laminated sediments. The laminated specimens, which form more than 75 per cent of the studied samples, show a higher degree of anisotropy, that is, $1.052 < Pj < 1.227$ than the remaining 25 per cent collected from massive facies which show a low anisotropy degree (such as $1.017 < Pj < 1.086$; a mean = 1.056).

Red bed samples of the Shaxian and Chongan Formations from the Southeast China Fold belt show a well-defined foliation in the AMS results and a lower degree of the corrected anisotropy ($1.008 < Pj < 1.107$).

Table 1. Late Cretaceous palaeomagnetic results from the Paomagang Formation at Yichang area, the middle part of the SCB.

Site	Longitude (°E)	Latitude (°N)	Strike (°)	Dip (°)	n	/	N	*in-situ* Decl. (°)	*in-situ* Incl. (°)	*in-situ* k	*in-situ* a_{95} (°)	Tilt corrected Decl. (°)	Tilt corrected Incl. (°)	Tilt corrected k	Tilt corrected a_{95} (°)	Polarity
North Paomagang																
* PM9	111°44′28″	30°43′01″	119	6	7	/	11	16.3	6.1	5.7	27.7	16.1	12.0	5.7	27.7	N
PM8	111°44′28″	30°43′13″	69	1	0	/	6									
PM7	111°44′25″	30°43′17″	153	3	4	/	8	39.8	15.9	4.5	48.6	39.3	18.5	4.5	49.1	N
	111°44′27″	30°43′15″														
PM6	111°44′28″	30°43′18″	11	16	2	/	11	8.1	7.6			8.3	6.7			N
			341	2												
* PM5	111°44′26″	30°43′20″	43	3	4	/	5	2.5	21.5	17.9	22.3	3.4	23.4	17.9	22.3	N
* PM4	111°44′25″	30°43′21″	57	7	9	/	11	0.1	18.4	28.9	9.7	1.6	24.2	28.9	9.7	N
* PM3	111°44′24″	30°43′23″	96	8	7	/	8	16.3	9.6	9.3	20.9	16.6	17.5	9.3	20.9	N
* PM2	111°44′24″	30°43′23″	67	8	12	/	13	349.9	−1.2	8.8	15.5	350.0	6.6	8.8	15.5	N
* PM1	111°44′24″	30°43′24″	94	11	5	/	10	355.7	22.7	12.8	22.2	354.8	33.6	12.8	22.2	N
Mean (*)					6			3.6	13.1	32.4	11.9	3.9	19.8	33.1	11.8	
South Paomagang																
* PM16	111°44′58″	30°42′23″	76	7	6	/	13	355.1	7.8	30.2	12.4	355.3	14.7	30.2	12.4	N
* PM15	111°44′55″	30°42′26″	84	12	5	/	7	11.6	21.5	22.5	16.5	13.6	32.9	22.5	16.5	N
* PM14	111°44′52″	30°42′27″	55	9	3	/	4	1.9	10.4	106.6	12.0	3.3	17.6	106.6	12.0	N
	111°44′52″	30°42′26″														
* PM13	111°44′51″	30°42′34″	25	5	5	/	8	11.2	37.3	10.5	24.8	15.0	38.3	10.5	24.8	N
	111°44′51″	30°42′32″														
* PM12	111°44′46″	30°42′39″	19	6	5	/	7	358.6	31.0	20.4	17.3	2.1	32.9	20.4	17.3	N
PM11	111°44′31″	30°42′47″	92	4	6	/	6	9.4	21.0	45.8	10.0	9.6	24.9	45.8	10.0	N
* PM10	111°44′29″	30°42′49″	79	8	7	/	8	355.0	42.8	8.6	21.8	356.0	50.8	8.6	21.8	N
Mean (*)					7		3.3	24.7	30.5	11.1	5.0	30.5	33.0	10.7		
Paomagang Mean (*)				13			3.4	19.3	28.9	7.9	4.5	25.6	31.0	7.6		
West Wangdian																
* WD1	111°41′17″	30°44′01″	181	53	8	/	13	4.5	4.8	16.7	14.0	0.1	7.2	16.8	13.9	N
			180	44												
WD2	111°41′19″	30°44′02″	176	34	1	/	10	348.0	29.4			332.5	19.8			N
WD3	111°41′19″	30°44′03″	178	28	1	/	7	29.9	5.2			24.5	19.1			N
* WD4	111°41′20″	30°44′04″	175	36	5	/	10	27.3	3.6	9.2	26.6	20.1	21.4	9.2	26.6	N/R
			171	26												
* WD5	111°41′20″	30°44′04″	171	26	7	/	7	20.8	4.8	65.8	7.5	16.3	17.0	65.8	7.5	N
* WD6	111°41′20″	30°44′04″	171	26	9	/	10	18.4	9.4	27.1	10.1	12.0	20.2	27.1	10.1	N/R
WD7	111°41′20″	30°44′05″	173	25	0	/	13									
* WD8	111°41′22″	30°44′08″	171	21	6	/	9	5.6	10.9	10.5	21.6	0.7	15.4	10.5	21.6	N
WD9	111°41′22″	30°44′09″	169	29	0	/	11									
WD10	111°41′23″	30°44′09″	160	28	0	/	12									
* WD11	111°41′23″	30°44′10″	159	25	6	/	10	20.6	5.1	55.2	9.1	16.0	21.1	55.2	9.1	N
WD12	111°41′23″	30°44′10″	122	34	0	/	8									
Mean (*)					6			16.2	6.5	71.8	8.0	10.7	17.2	68.8	8.1	
East Wangdian																
SM15	111°42′24″	30°44′05″	272	17	0	/	5									
SM14	111°42′24″	30°44′04″	208	12	5	/	6	39.9	-3.4	7.5	29.9	40.3	-0.9	7.5	29.9	N/R
* SM13	111°42′13″	30°44′27″	83	15	9	/	9	14.3	31.4	12.9	14.9	18.3	36.6	15.9	13.3	N
	111°42′14″	30°44′25″	23	6												
SM12	111°42′06″	30°44′32″	7	13	0	/	6									
	111°42′09″	30°44′29″	24	6												
	111°42′10″	30°44′29″	15	5												
* SM11	111°42′03″	30°44′37″	19	7	5	/	8	347.6	28.8	27.8	14.8	351.2	32.2	27.8	14.8	N
Mean (*)					2			0.8	30.8			4.4	35.2			
North Wangdian																
* WD14	111°41′40″	30°44′48″	75	1	6	/	10	355.7	11.2	13.0	19.3	355.8	12.2	13.0	19.3	N
WD13	111°41′41″	30°44′49″	305	1	0	/	6									
* WD15	111°41′49″	30°44′52″	96	1	9	/	14	344.7	22.2	61.7	6.6	344.6	23.2	61.7	6.6	N
SM10	111°41′47″	30°44′46″	106	4	1	/	16	10.9	28.6			10.7	32.6			N
	111°41′48″	30°44′46″														
	111°41′49″	30°44′46″	325	8												
* SM9	111°41′42″	30°44′47″	82	7	8	/	14	349.4	27.9	102.7	5.5	349.2	34.9	102.7	5.5	N
* SM8	111°42′01″	30°44′56″	343	1	4	/	4	356.3	18.2	33.7	16.1	356.6	17.9	33.7	16.1	N

Table 1. (*Continued.*)

Site	Longitude (°E)	Latitude (°N)	Strike (°)	Dip (°)	n	/	N	*in-situ* Decl. (°)	*in-situ* Incl. (°)	*k*	a_{95} (°)	Tilt corrected Decl. (°)	Tilt corrected Incl. (°)	*k*	a_{95} (°)	Polarity
SM7	111°41′59″	30°44′57″	342	10	1	/	5	5.8	26.4			9.9	22.0			N
SM6	111°41′56″	30°44′57″	332	13	1	/	6	9.3	26.0			13.3	17.8			N
* SM5	111°41′51″ 111°41′53″	30°44′58″ 30°45′00″	316	5	4	/	9	358.9	12.8	55.1	12.5	359.6	9.3	55.1	12.5	R
Mean (*)					5			353.1	18.5	85.4	8.3	353.4	19.6	48.7	11.1	
Wangdian Mean (*)					13			5.3	15.1	23.3	8.8	3.1	21.0	31.8	7.5	

Formation Mean	*n*	*in-situ* Decl. (°)	*in-situ* Incl. (°)	*k*	a_{95} (°)	Tilt corrected Decl. (°)	Tilt corrected Incl. (°)	*k*	a_{95} (°)
Paomagang + Wangdian	26	4.4	17.2	26.3	5.6	3.8	23.3	31.8	5.1

Virtial Geomagnetic Pole	Longitude (°E)	Latitude (°N)	*k*	A_{95} (°)
Paomagang + Wangdian	280.0	71.5	45.0	4.3

Magnetization directions of the high temperature component are listed for two areas, Paomagang and Wangdian. In this table, N and n are the number of specimens measured and used for calculation, respectively. Mean directions for all sampling sites of the Paomagang Formation and for each area (Paomagang and Wangdian) are calculated on the basis of palaeomagnetic directions at the representative location of Yichang (30.7°N, 111.7°E). Dec. and Inc. are declination and inclination respectively; k and α_{95} are the estimate of the Fisherian precision parameter and the radii of cone of 95 per cent confidence (Fisher 1953). Data denoted by asterisk are used for calculation of formation and area mean directions. Strikes of bedding are listed after the subtraction of local geomagnetic declination calculated using the International Geomagnetic Reference Field (Mandea & Macmillan 2000), Palaeomagnetic results from the Paomagang formation.

5 PALAEOMAGNETIC RESULTS

Initial NRM intensities of the studied red beds varied between 5.6 $\times$ 10^{-3} and 1.9 $\times$ 10^{-2} A m^{-1}. No significant enhancement was observed in the magnetic susceptibility during stepwise heating, which indicates the lack of mineralogical transformation during the thermal demagnetization. Progressive thermal demagnetization up to 690°C generally revealed two remanent components (Fig. 5). The low temperature component (LTC) was generally removed by 350°C. A LTC similar to the present geomagnetic field direction was often observed in samples, which gave a reversed polarity high temperature component (HTC) in geographic coordinates.

The HTC was unblocked in a range between 400°C and 690°C, indicating haematite as a remanence carrier. The HTC is isolated from 34 out of 42 sites. Erratic demagnetization behaviour precluded an identification of remanent directions in the remaining eight sites (one site of the Paomagang area and seven sites of the Wangdian area).

The HTC, which we consider as a characteristic component, has dual polarity directions. 30 out of 34 sites are of normal polarity (Fig. 6), where *in situ* remanent directions are characterized by northerly declination and shallow inclination. Site mean directions from 23 sites show good clustering with associated precision parameter values between 5.7 and 106.6 (Table 1). The data of the remaining seven sites with normal polarity are not recognized as reliable ones because of a small number of samples ($n < 2$) per site (PM6, WD2, WD3, SM10, SM6 and SM7) or large 95 per cent confidence circle ($\alpha_{95} = 49.1°$; PM7).

The remaining four sites with multi-layers strata (WD4, WD6, WD14 and SM5) include reversed polarity directions (Fig. 7). Remanent directions from all layers of the site SM5 are of reversed polarity and are antipodal to those of normal polarity in other 30 sites. This type of behaviour indicates that a complete record of reversed polarity is preserved in the rocks of this site. Two other sites (WD4 and WD6) have a reversed polarity direction in only one layer, which is antipodal to those of normal polarity from other layers in the same sites. A site mean direction of these sites is calculated after inverting a reversed polarity into normal one (Table 1). In contrast, we interpret the remaining one site (SM14) to have recorded a geomagnetic image during an excursion, because the remanent directions are positioned on a great circle. The lowest two layers show a southwesterly and upward direction, whereas the successive stratigraphically higher layers show northeasterly and upward directions. Because of these factors the results from site SM14 were excluded from the data used to calculate the formation mean direction. In summary, 26 sites have reliable HTC directions, including 23 sites with normal polarity, one site with reversed polarity and two sites with dual polarities.

6 ANALYSIS OF PALAEOMAGNETIC RESULTS

Formation mean direction of the HTC is calculated using 13 sites of the Paomagang locality. After tilt correction, grouping of the mean directions slightly improves ($k_2/k_1 = 31.0/28.9$) (Table 1; Fig. 6), with the observed tilt-corrected mean direction of $Dc = 4.5°$, $Ic = 25.6°$, $\alpha_{95} = 7.6°$, $N = 13$. In the study region, the bedding attitude slightly varies through the stratigraphic sequence, although Late Cretaceous strata in the Paomagang area form monoclinal structure. We, therefore, applied the second definition (ξ_2) in the method of McFadden (1990) to examine the fold test for the 13 sites. The fold test is positive at the 95 per cent confidence level, where the calculated value (ξ_2) is 5.620 in geographic coordinates and 2.143 in stratigraphic coordinates, while the critical value (ξ) is 4.200 at 95 per cent confidence level.

Additionally, we selected several sets of sampling sites for further fold test where differences of bedding attitudes are the largest in all sites. A subset of six sites from the North Paomagang locality (PM1–PM5, PM9) passed the McFadden (1990) fold test at 95 per cent significance. Therefore, we conclude that the Late Cretaceous remanent magnetization from the Paomagang area is primary in origin.

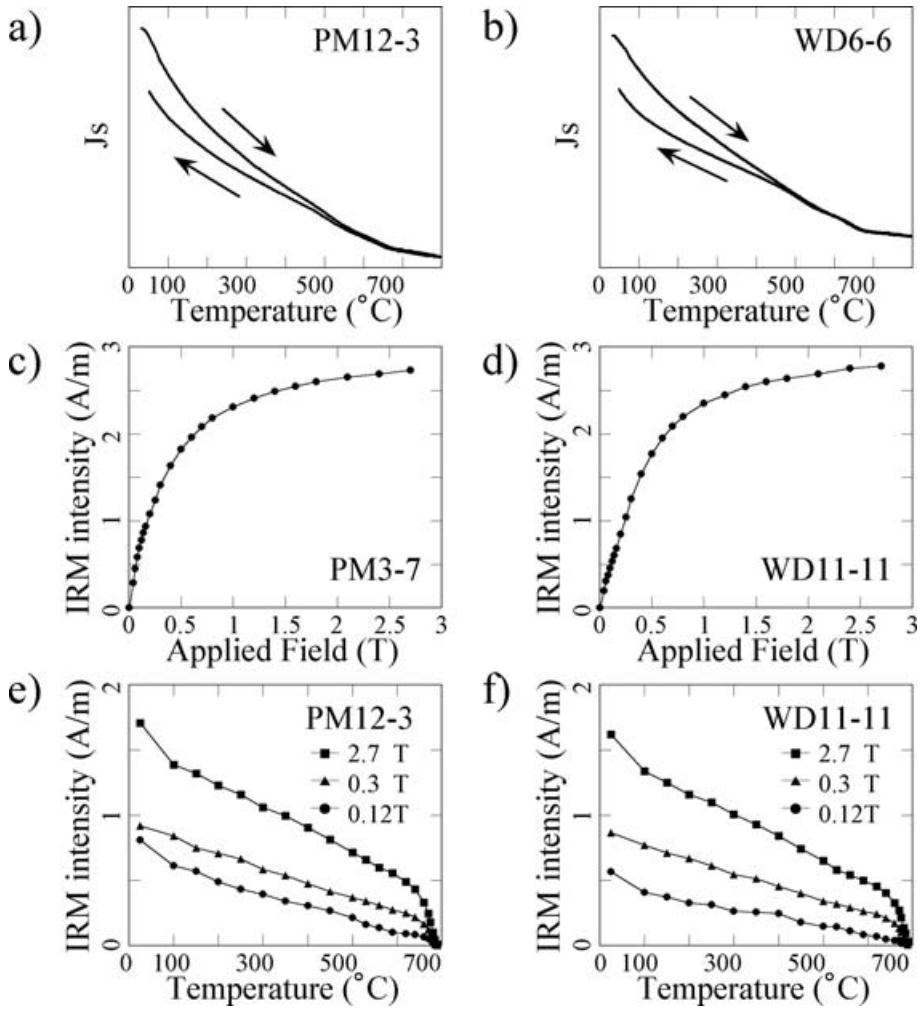

Figure 3. Rock magnetic experiments on selected specimen from Paomagang Formation. (a), (b); High field saturation magnetization (*Js*) versus temperature curves for the samples of Paomagang and Wangdian areas. Thermomagnetic analyses were performed in air. The arrows indicate heating and cooling curves. (c), (d); IRM acquisition curves (closed circles) for the representative specimens. (e), (f); IRMs of different DC fields (2.7T, 0.4T and 0.12T) were imparted along each of three perpendicular axes. These composite IRMs were then thermally demagnetized.

For the Wangdian area, 13 sites provide a tilt-corrected formation mean direction (after inverting a reversed polarity direction into normal one) of $Dc = 3.1^\circ, Ic = 21.0^\circ, \alpha_{95} = 7.5^\circ, N = 13$. Grouping of the formation mean direction improves after applying the tilt correction ($k_2/k_1 = 31.8/23.3$), although the fold test of McFadden formulation (1990) for the 13 sites is inconclusive. Because strata at the West Wangdian locality is dipping westward and those at the North Wangdian towards the northeast, two sets of data were available for applying the first definition (ξ_1) in the method of McFadden (1990) to examine the fold test. Taking in to consideration 11 sites from West Wangdian locality (WD1, WD4, WD5, WD6, WD8 and WD11) and North Wangdian locality (WD14, WD15, SM9, SM8 and SM5), the fold test is positive at the 95 per cent confidence level. For this test, a calculated value (ξ_1) is 4.102 in geographic coordinates and 1.871 after application of the tilt correction, while the critical value (ξ) is 3.865 at the 95 per cent confidence level.

Relatively continuous collection of samples between sites SM5 and SM8 of the North Wangdian shows a normal to reverse polarity magnetostratigraphic sequence in ascending order. The McFadden & McElhinny (1990) reversal test is applied to one reversed polarity (SM5) and 12 other normal polarity sites. This test gives a γ_c value of 28.3°, while the difference between normal and antipodal reversed mean directions is 13.2°, indicating that a reversal test is passed at the 95 per cent confidence level with a 'I' classification.

We interpret these observations to indicate that the HTC in Wangdian area samples preserved a primary remanent magnetization similar to the remanent magnetization determined from samples calculated from the Paomagang area. Because the formation mean direction for the Wangdian area is indistinguishable at the 95 per cent confidence level from that of the Paomagang area (the difference in direction is $4.6^\circ \pm 10.6^\circ$), we combined all 26 sites from both areas and estimated an overall tilt-corrected characteristic mean direction of $Dc = 3.8^\circ, Ic = 23.3^\circ$, with $\alpha_{95} = 5.1^\circ$.

Taking into consideration the AMS data and sedimentary characteristics, a formation mean direction was calculated on the basis of two groups consisting of samples with laminated and massive facies (Fig. 8). Assigning unit weight to each site, the tilt-corrected formation mean directions for laminated and massive samples are $Dc = 4.9^\circ, Ic = 22.7^\circ$, with $\alpha_{95} = 6.6^\circ$ and $Dc = 11.5^\circ, Ic = 29.3^\circ$, with $\alpha_{95} = 6.1^\circ$, respectively. A set of laminated sites gave an inclination value of $6.6^\circ \pm 9.0^\circ$ shallower than the massive ones.

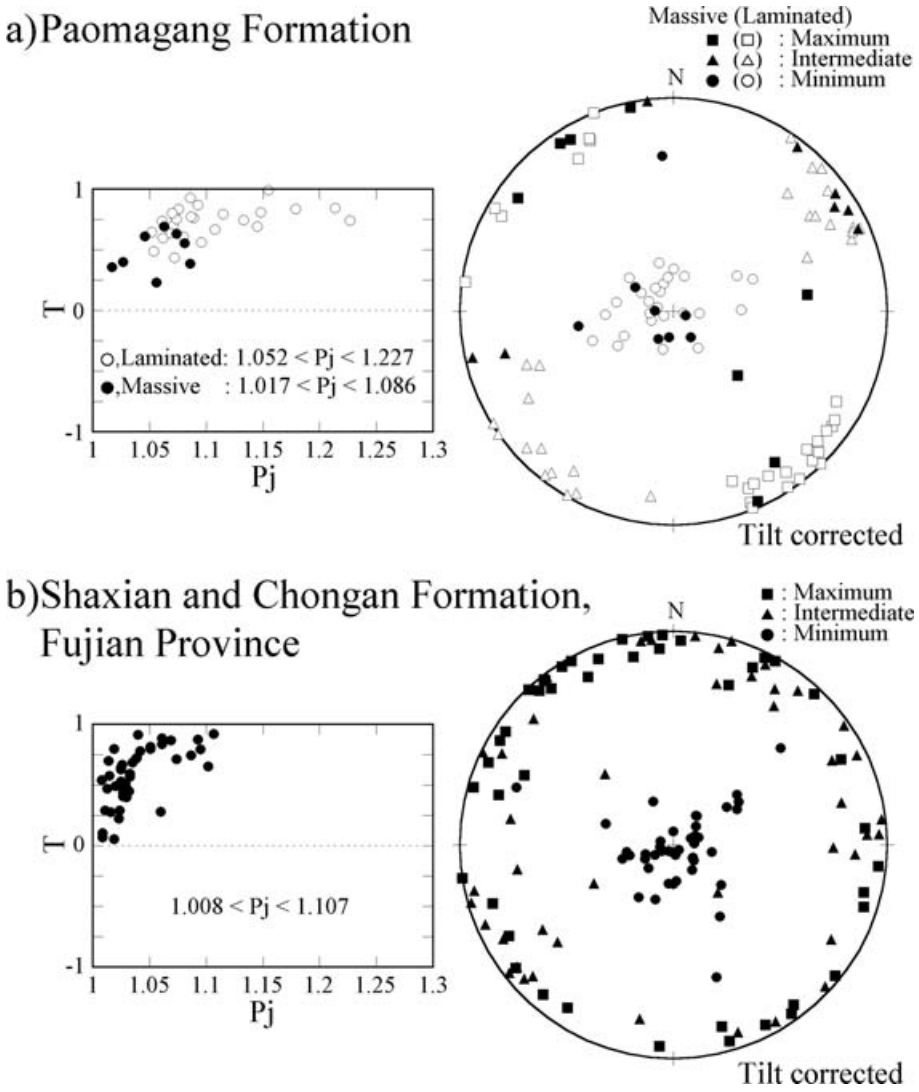

Figure 4. The principal directions of susceptibility together with plots of shape parameter (T) and the degree of anisotropy (*Pj*) (a) results of the Paomagang Formation from Paomagang area and (b) results for Shaxian and Chongang formations from Fujian province. The principal directions are projected onto the lower hemisphere (Equal-area projection). Squares are maximum susceptibility direction (K_1); Triangles are intermediate susceptibility directions (K_2); Circles are minimum susceptibility directions (K_3). Closed (open) symbols in the Paomagang Formation represent data for massive (laminated) samples.

7 DISCUSSION

We have defined the first Late Cretaceous palaeomagnetic results from the Yichang area in the mid-northern portion of the SCB. We interpret the primary origin of this data by the observational positive fold and reversal tests. The mean tilt-corrected characteristic palaeomagnetic direction for this study is $Dc = 3.8^\circ$, $Ic = 23.3^\circ$, with $\alpha_{95} = 5.1^\circ$ and the corresponding palaeopole is $\lambda = 71.5^\circ$N, $\phi = 280.0^\circ$E, $A_{95} = 4.3^\circ$ (Fig. 1a).

We compare the tilt-corrected Yichang pole with a reference Cretaceous pole for the stable SCB. A Cretaceous pole recently reported by Morinaga & Liu (2004) (80.0°N, 206.7°E, $A_{95} = 2.5^\circ$) is adopted as the reference pole because their selected poles for calculation are distributed in the eastern side of the SCB as well as the in the western side of the SCB. The Late Cretaceous palaeomagnetic pole from Yichang is far sided with respect to the reference pole. The angular separation is $18.2^\circ \pm 5.0^\circ$ between the tilt-corrected Yichang pole and reference SCB pole.

The far-sided nature of pole positions for the Yichang area is the outcome of observed inclinations, which are shallower than the expected palaeomagnetic field inclination calculated from APWPs for the SCB and Eurasia Plate. Inclination flattening is $25.0^\circ \pm 5.9^\circ$ and $26.3^\circ \pm 6.4^\circ$ at the Yichang area with respect to the expected inclination for the stable body of SCB and Eurasia at 80 Ma (76.2°N, 198.9°E, $A_{95} = 3.4^\circ$; Besse & Courtillot 1991), respectively.

Although the SCB behaved as a rigid block within the associated palaeomagnetic uncertainty (Morinaga & Liu 2004), middle Cretaceous to Cenozoic NW–SE extension within the SCB is suggested on the basis of local and regional evidences dominated by grabens, pull-apart basins and basaltic magmatism (Tian *et al.* 1992; Zhou & Li 2000; Ren *et al.* 2002; Zhu *et al.* 2004). The inclination flattening can be partly ascribable to north–south extension between Yichang area and Southeast China Fold Belt. The present distance between the Yichang area and Southeast China Fold Belt is about 1000 km, while the JHB (Fig. 1) occupies one-fifth of this distance between them. Assuming that the JHB were formed by the Tertiary

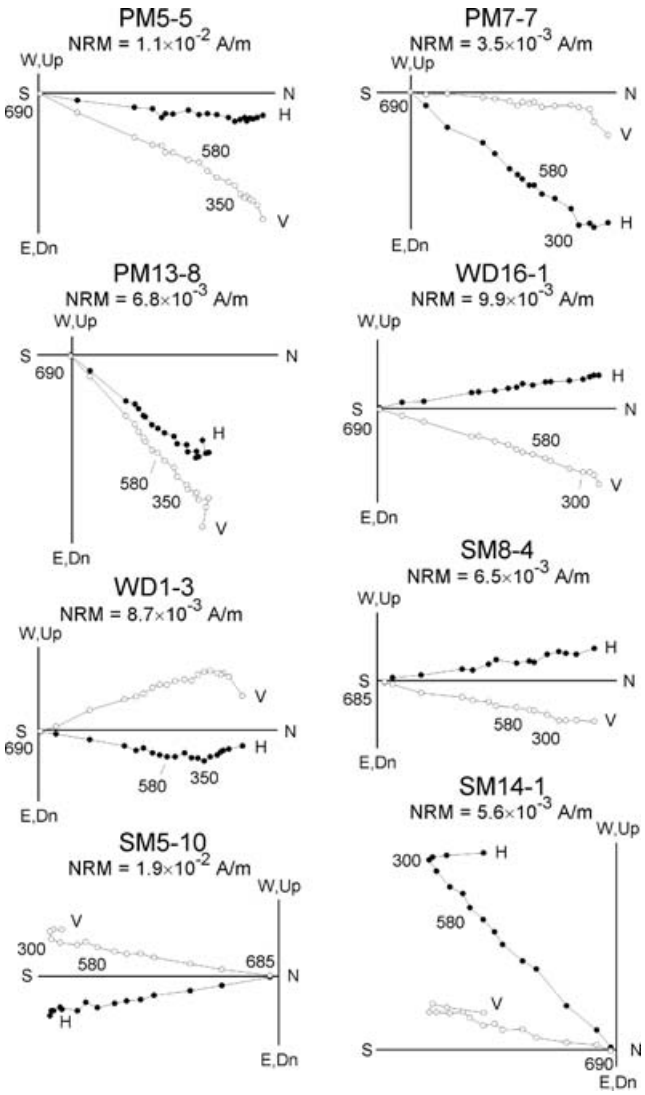

Figure 5. Orthogonal vector plots (Zijderveld diagrams) for the samples of Paomagang Formation after thermal demagnetization. PM7, PM13 and PM16 are from the Paomagang area, and SM8, SA5, WD1, WD6 and SM14 are from the Wangdian area. Numbers adjacent to demagnetization path are step heating temperatures in degree Celsius. Open (solid) symbols show projection on to vertical (horizontal) plane. All directions are plotted in geographic coordinates.

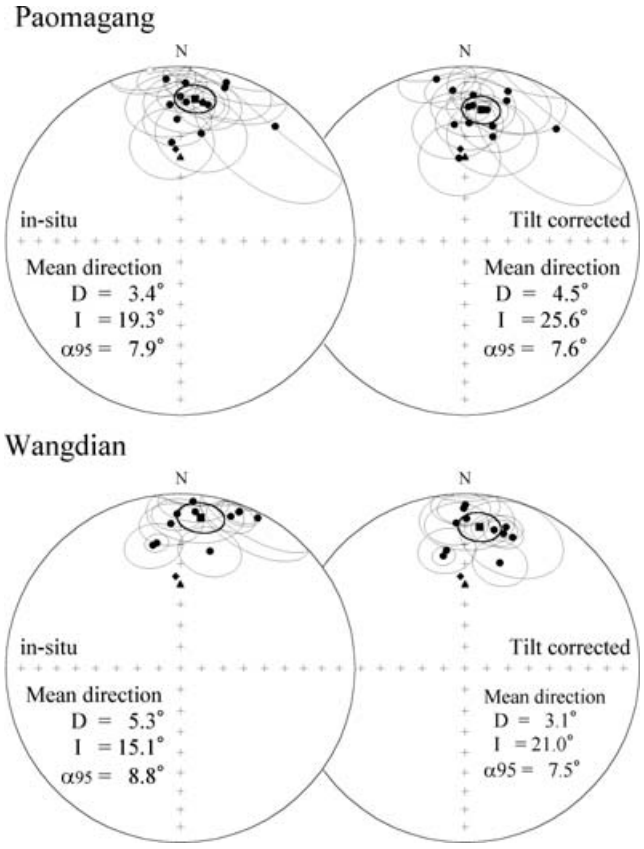

Figure 6. Equal-area projections of the site mean directions with 95 per cent confidence circle for the Paomagang and Wangdian areas. Three site mean directions with reversed polarity from the Wangdian area are shown after inverting them to normal polarity. The square symbol with associated-shaded circle of confidence indicates the overall mean direction. Solid symbols are projections on to the lower hemisphere. Diamond and triangle symbols are the present geomagnetic field direction and axial geocentric dipole field, respectively.

rifting (Ren *et al.* 2002), displacement would not exceed the width of 200 km of the basin (1.8° in latitude) and contributes at the most 2.0° to inclination flattening.

The shallowing of inclination may be due to geomagnetic field and/or rock magnetic effects (Gilder *et al.* 2001). In case of geomagnetic field, the strength of geocentric axial dipole is usually added by the contribution of non-dipole field (Wilson 1971; Kent & Smethurst 1998) or a stationary non-dipole component beneath an anomalously shallow inclination region (e.g. Mongolian anomaly; Yukutake & Tachinaka 1968). The former geomagnetic field phenomenon is of global scale, while the latter one is of regional scale. However, no shallow inclination values of global and regional scales have been recorded in the Late Cretaceous–Cenozoic igneous rocks of the SCB and Tarim Basin. Upper Cretaceous dikes from Hong Kong reveal insignificant inclination flattening (6.6° ± 14.5°) with respect to the expected inclination value from the Eurasia APWP (Li *et al.* 2005). No significant inclination anomaly is reported from Palaeogene and Pleistocene basalt flows of the Tien Shan and Kunlun areas of central Asia (Otofuji *et al.* 1995; Bazhenov & Mikolaichuk 2002). Therefore, the geomagnetic field can not explain the substantially shallow inclinations observed in the Yichang area.

Another possible explanation for the observed shallow inclinations is depositional-induced inclination shallowing in the samples of red beds (Garces *et al.* 1996; Tan & Kodama 2002; Tan *et al.* 2003). Observed correlation of tilt-corrected inclination to magnetic anisotropy and sedimentary facies suggests that a depositional environment is responsible for the observed shallowing. Fig. 9 shows inclinations of samples from the Paomagang Formation at the Yichang area plotted as a function of anisotropy degree (Pj). The most suitable line is $I = 29.8 - 71.7(Pj - 1)$. Although a correlation coefficient is small as -0.248, negative association is observed between inclination and anisotropy degree. The anisotropy becomes larger, inclination approaches to less than 15 degrees. In addition, rocks of laminated red beds in the Paomagang Formation reveal a high degree of anisotropy ($1.052 < Pj < 1.227$) and shallow inclination ($I = 22.7°$; inclination flattening with respect to Eurasian pole = $26.9° \pm 7.6°$), whereas those from massive facies show a low degree of anisotropy ($1.017 < Pj < 1.086$) with steep inclination ($I = 29.3°$; inclination flattening = $20.3° \pm 7.2°$) (Figs 4 and 8). Also, the palaeomagnetic pole of the Late Cretaceous red bed samples of the

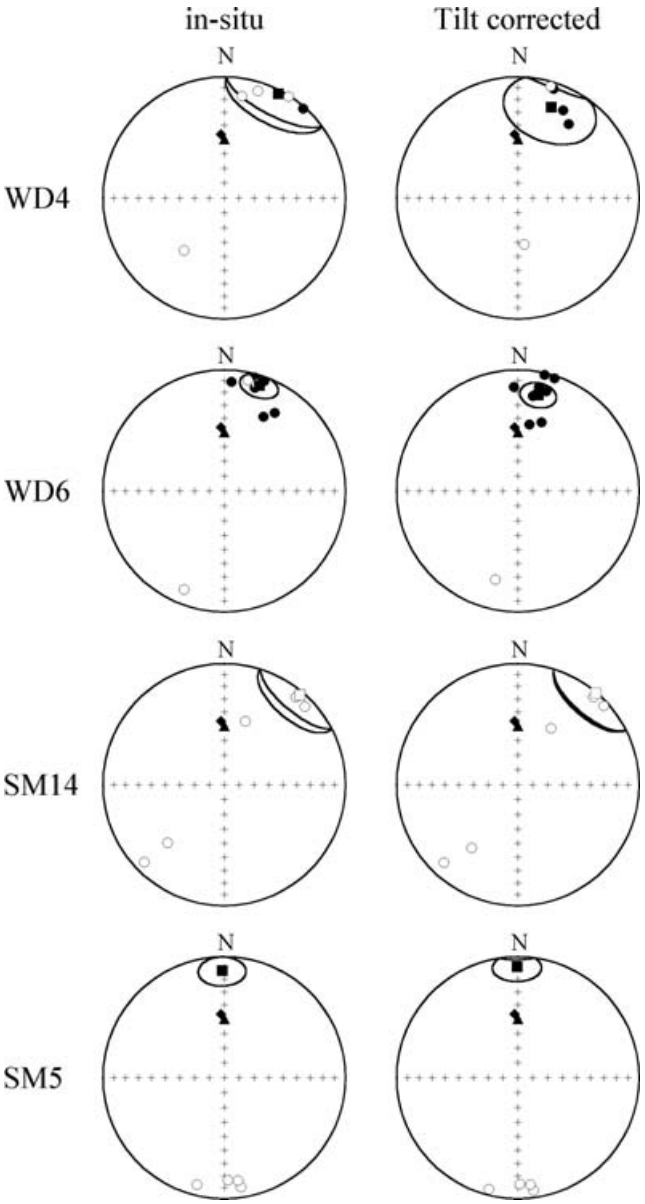

Figure 7. Equal-area projections of the remanent directions for four sites (WD4, WD6, WD14 and SM5). Four sites have a layer or layers with reversed polarity direction. Remanent directions in all layers of site SM5 are of reversed polarity and are antipodal to the other normal polarity sites. Sites WD4 and WD6 have a reversed polarity direction in only one layer. Direction of this reversed polarity layer is antipodal to other normal polarity layers from the same site. Site SM14 seems to have recorded a geomagnetic record during excursion. Square with shaded circle of confidence indicates the overall site mean direction. Solid (open) symbols are lower (upper) hemisphere directions. Diamond and triangle symbols represent geomagnetic field direction and axial geocentric dipole field, respectively.

Shaxian and Chongan Formations in the Southeast China Fold Belt is consistent with contemporaneous palaeomagnetic poles of NCB and Eurasia (Morinaga & Liu 2004). Red bed samples from these formations show no inclination flattening ($1.5^\circ \pm 6.9^\circ$ with respect to Eurasian pole) and a low degree of the anisotropy ($1.008 < Pj < 1.107$). Massive samples selected from these samples reveal an even lower degree ($1.008 < Pj < 1.040$) of anisotropy.

This implication can quantitatively be confirmed because similar inclination flattening between 15° and 30° is observed in red beds of the Valles-Penedes Basin, where a high degree of anisotropy ($1.150 < Pj < 1.250$) is reported from the laminated rocks (Garces *et al.* 1996). We conclude that inclination flattening of about 25° from the Yichang area should be attributed to depositional-induced inclination shallowing.

Comparing the observed declination at Yichang with the expected one calculated from the reference pole for the stable SCB, counter-clockwise deflected palaeomagnetic declination is found. The Yichang area was probably subjected to the tectonic rotation by $-7.6^\circ \pm 6.2^\circ$ later than the Late Cretaceous with respect to the stable SCB. Regional extent and tectonic origin of this counter-clockwise rotational motion is the future subject in the middle–northern part of the SCB.

8 CONCLUSION

A shallow inclination is observed in the red beds of the Paomagang Formation. Inclination flattening in the observed tilt-corrected palaeomagnetic direction is $26.3^\circ \pm 6.4^\circ$ with respect to that expected from the 80 Ma pole of the SCB or Eurasia. Good correlation among the amount of inclination flattening, the degree of anisotropy and sedimentary facies indicates that the depositional processes produced the observed shallow inclination in the Yichang area. Because the far-sided pole position (78.6°N, 273.4°E, $dp/dm = 2.4^\circ/4.1^\circ$) is reported from Cretaceous red beds in the Sichuan basin in the SCB (Otofuji *et al.* 1990; Enkin *et al.* 1991a,b), further palaeomagnetic and rock magnetic studies are required to study the shallowing effect in this basin.

ACKNOWLEDGMENTS

We wish to express our gratitude to Prof Naoto Ishikawa of the Graduate School of Human and Environmental Studies, Kyoto University for offering their rock and palaeomagnetic laboratory. We also thank Drs W. Harbert and X.D. Tan for their critical reviews on the manuscript. This work was supported in part by the Sasagawa Foundation, the Toyota Foundation, Grant-in-aid for Scientific Research (B) from the Japan Society for the Promotion of Science (No. 14403010) and by 'The 21st Century COE Program of Origin and Evolution of Planetary Systems' in Japanese Ministry of Education, Culture, Sports, Science and Technology (MEXT). This work was also partly supported a NNSF grant 49925410 to ZY.

REFERENCES

Bazhenov, M.L. & Mikolaichuk, A.V., 2002. Paleomagnetism of Paleogene basalts from the Tien Shan, Kyrgystan: rigid Eurasia and dipole geomagnetic field, *Earth planet. Sci. Lett.,* **195,** 155–166.

Besse, J. & Courtillot, V., 1991. Revised and synthetic apparent polar wander paths of the African, Eurasian, North American and Indian plates, and true polar wander since 200 Ma, *J. geophys. Res.,* **96,** 4029–4050.

Bureau of Geology and Mineral Resources of Hunan province (BGMRHN), 1988. Regional geology of Hunan province, Geological Publishing House, Beijing, China.

Chauvin, A., Perroud, H. & Bazhenov, M.L., 1996. Anomalous low palaeomagnetic inclinations from Oligocene-Lower Miocene red beds of the south-west Tien Shan, Central Asia, *Geophys. J. Int.,* **126,** 303–313.

Chen, Y. et al, 1991. Paleomagnetic study of Mesozoic continental sediments along the Northern Tien Shan (China) and heterogeneous strain in Central Asia, *J. geophys. Res.,* **96,** 4065–4082.

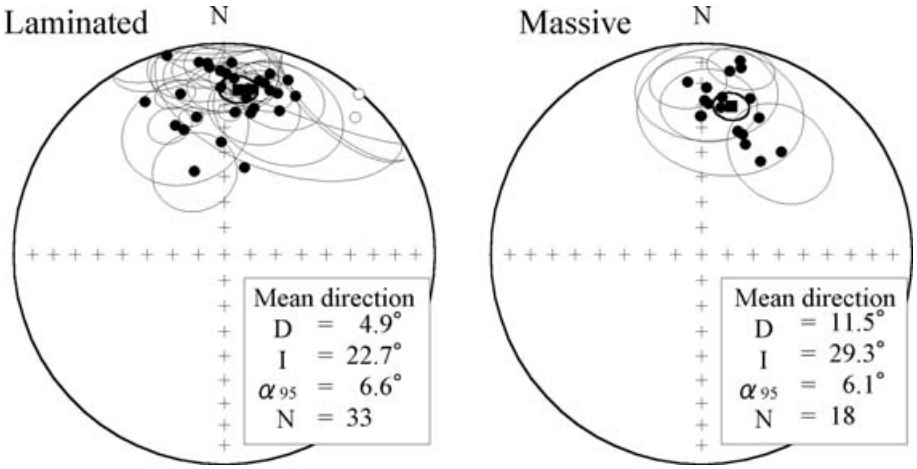

Figure 8. Equal-area projections of the site mean directions (with 95 per cent confidence circle) for laminated and massive samples from the Paomagang Formation after tilt correction. Solid (open) symbols are lower (upper) hemisphere directions. Mean direction: the tilt-corrected formation mean directions are computed using Fisherian statistics (Fisher 1953) assigning unit weight to each site. *N* is the number of sites. While laminated samples were observed in 33 sites, massive samples only appeared in 18 sites.

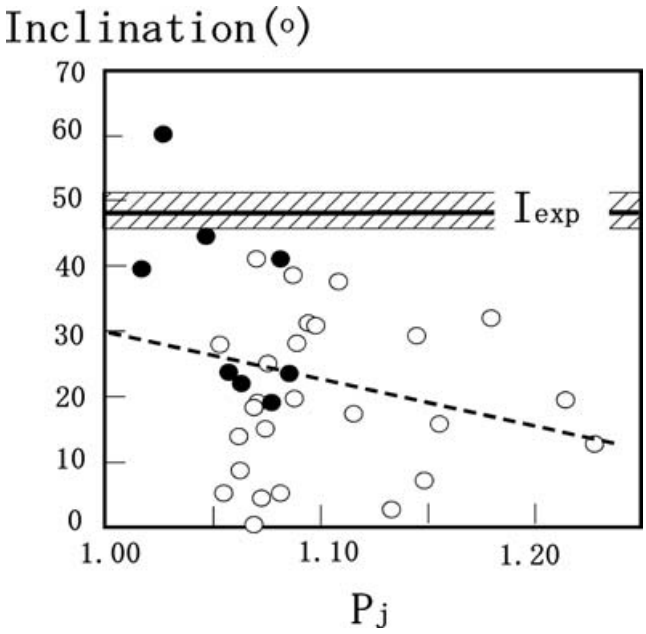

Figure 9. Relationship between tilt-corrected inclination and degree of anisotropy (*Pj*) for samples from the Paomagang Formation at Yichan. Open and closed circles are laminated and massive samples, respectively. Expected inclination and its 95 per cent confidence interval (Iexp $= 48.3^\circ \pm 2.9^\circ$) at Yichang are shown by black line and shaded area, which are calculated from the palaeopole of the SCB (80.0°N, 206.7°E, $A_{95} = 2.5^\circ$). A broken line shows the most fitted straight line of inclination as a function of the degree of anisotropy; $I = 29.8 - 71.7(Pj - 1)$. A correlation coefficient is −0.248.

Chen, Y., Cogne, J.P. & Courtillot, V., 1992. New Cretaceous paleomagnetic poles from the Tarim basin, northwestern China, *Earth planet. Sci. Lett.,* **114,** 17–38.

Chen, Y., Wu, H., Courtillot, V. & Gilder, S., 2002. Large N-S convergence at the northern edge of the Tibetan plateau? New Early Cretaceous paleomagnetic data from Hexi Corridor, NW China, *Earth planet. Sci. Lett.,* **201,** 293–307.

Cogne, J.P., Halim, N., Chen, Y. & Courtillot, V., 1999. Resolving the problem of shallow magnetizations of Tertiary age in Asia: insights from paleomagnetic data from the Qiangtang, Kunlun, and Qaidam blocks (Tibet, China), and a new hypothesis, *J. geophys. Res.,* **104,** 17 715–17 734.

Enkin, R.J., Chen, Y., Courtillot, V., Besse, J., Xing, L., Zhang, Z., Zhuang, Z. & Zhang, J., 1991a. Cretaceous pole from south China, and the Mesozoic hairpin turn of the Eurasia apparent polar wander path, *J. geophys. Res.,* **96,** 4007–4027.

Enkin, R.J., Courtillot, V., Xing, L., Zhang, Z., Zhuang, Z. & Zhang, J., 1991b. The stationary Cretaceous paleomagnetic pole of Sichuan (South China Block), *Tectonics.,* **10,** 547–559.

Enkin, R.J., Yang, Z.Y., Chen, Y. & Courtillot, 1992. Paleomagnetic constraints on the Geodynamic history of the major blocks of China from the Permian to the Present, *J. geophys. Res.,* **97,** 13 953–13 989.

Fisher, R., 1953. Dispersion on a sphere, *Proc. R. Soc. London, Ser. A,* **217,** 295–305.

Garces, M., Pares, J.M. & Cabrera, L., 1996. Further evidence for inclination shallowing in red beds, *Geophys. Res. Lett.,* **23,** 2065–2068.

Gilder, S.A., Coe, R.S., Wu, H., Kuang, G., Zhao, X., Wu, Q. & Tang, X., 1993. Cretaceous and Tertiary paleomagnetic results from Southeast China and their tectonic implications, *Earth planet. Sci. Lett.,* **117,** 637–652.

Gilder, S.A. et al, 1996. Isotopic and paleomagneitc constraints on the Mesozoic tectonic evolution of south China, *J. geophys. Res.,* **101,** 16 137–16 154.

Gilder, S.A. et al, 1999. Tectonic evolution of the Tancheng-Lujiang (Tan-Lu) fault via Middle Triassic to Early Cenozoic paleomagnetic data, *J. geophys. Res.,* **104,** 15 365–15 390.

Gilder, S., Chen, Y. & Sen, S., 2001. Oligo-Miocene magnetostratigraphy and rock magnetism of the Xishuigou section, Subei (Gansu Province, western China) and implications for shallow inclinations in central Asia, *J. geophys. Res.,* **106,** 30 505–30 521.

Houseman, G. & England, P., 1986. Finite strain calculations of continental deformation 1. Method and general results for convergent zones, *J. geophys. Res.,* **91,** 3651–3663.

Kent, D.V. & Smethurst, M.A., 1998. Shallow bias of paleomagnetic inclinations in the Paleozoic and Precambrian, *Earth planet. Sci. Lett.,* **160,** 391–402.

Kirschvink, J.L., 1980. The least-squares line and plane and the analysis of palaeomagnetic data, *Geophys. J. R. astr. Soc.,* **62,** 699–718.

Li, Z.X., 1998. Tectonic history of the major East Asian lithospheric blocks since the Mid-Proterozoic—a synthesis, in *Mantle Dynamics and Plate Interactions in East Asia*, pp. 221–243, eds Flower, M.F.J., Chung, S-L., Lo, C-H. & Lee, T.-Y., Geodynamics Series 27, AGU, Washington D.C.

Li, Y., Zhang, Z., McWilliams, M., Sharps, R., Zhai, Y., Li, Y., Li, Q. & Cox, A., 1988. Mesozoic paleomagnetic results of the Tarim craton: Tertiary relative motion between China and Siberia?, *Geophys. Res. Lett.,* **15,** 217–220.

Li, Y., Ali, J.R., Chan, L.S. & Lee, C.M., 2005. New and revised of Cretaceous paleomagnetic poles from Hong Kong: implications for the development of southeast China, *Jour. Asian Earth Sci.,* **24,** 481–493.

Lowrie, W., 1990. Identification of ferromagnetic minerals in a rock by coercivity and unblocking temperature properties, *Geophys. Res. Lett.,* **17,** 159–162.

Mandea, M. & Macmillan, S., 2000. International geomagnetic reference field—the eighth generation, *Earth Planets Space,* **52,** 1119–1124.

McFadden, P.L., 1990. A new fold test for palaeomagnetic studies, *Geophys. J. Int.,* **103,** 163–169.

McFadden, P.L. & McElhinny, M.W., 1990. Classification of the reversal test in palaeomagnetism, *Geophys. J. Int.,* **130,** 725–729.

Morinaga, H. & Liu, Y., 2004. Cretaceous paleomagnetism of the eastern South China Block: establishment of the stable body of SCB, *Earth planet. Sci. Lett.,* **222,** 971–988.

Otofuji, Y., Inoue, Y., Funahara, S., Murata, F. & Zheng, X., 1990. Palaeomagnetic study of eastern Tibet—deformation of the Three Rivers region, *Geophys. J. Int.,* **103,** 85–94.

Otofuji, Y., Itaya, T., Wang, H.C. & Nohda, S., 1995. Palaeomagnetism and K-Ar dating of Pleistocene volcanic rocks along the Altyn Tagh fault, northern border of Tibet, *Geophys. J. Int.,* **120,** 367–374.

Ren, J., Tamaki, K., Li, S. & Junxia, Z., 2002. Late Mesozoic and Cenozoic rifting and its dynamic setting in Eastern China and adjacent areas, *Tectonophys.,* **344,** 175–205.

Tan, X. & Kodama, K.P., 2002. Magnetic anisotropy and paleomagnetic inclination shallowing in red beds: evidence from the Mississippian Mauch Chunk Formation, Pennsylvania, *J. geophys. Res.,* **107**(B11), 2311, doi:10.1029/2001JB001636.

Tan, X., Kodama, K.P., Chen, H., Fang, D., Sun, D. & Li, Y., 2003. Paleomagnetism and magnetic anisotropy of Cretaceous red beds from the Tarim basin, northwest China: evidence for a rock magnetic cause of anomalously shallow paleomagnetic inclinations from central Asia, *J. geophys. Res.,* **108**(B2), 2107, doi:10.1029/2001JB001608.

Tapponnier, P., Peltzer, G., Le Dain, A.Y., Armijo, R. & Cobbold, P., 1982. Propagating extrusion tectonics in Asia: new insights from simple experiments with plasticine, *Geology,* **10,** 611–616.

Tarling, D.H. & Hrouda, F., 1993. *The magnetic anisotropy of rocks*, Chapman & Hall, London, 14–28.

Thomas, J.C., Perroud, H., Cobbold, P.R., Bazhenov, M.L., Burtman, V.S., Chauvin, A. & Sadybakasov, E., 1993. A paleomagnetic study of Tertiary formations from the Kyrgyz Tien-Shan and its tectonic implications, *J. geophys. Res.,* **98,** 9571–9589.

Tian, Z.Y., Han, P. & Xu, K.D., 1992. The Mesozoic-Cenozoic East China rift system, *Tectonophys.,* **208,** 341–363.

Westphal, M., Bazhenov, M.L., Lauer, J.P., Pechersky, D.M. & Sibuet, J-C., 1986. Paleomagnetic implications on the evolution of the Tethys belt from the Atlantic Ocean to the Pamirs since the Triassic, *Tectonophys.,* **123,** 37–82.

Wilson, R.L., 1971. Dipole offset - the time averaged palaeomagnetic field over the past 25 million years, *Geophys. J. R. astr. Soc.,* **22,** 491–504.

Yang, Z.Y. & Besse, J., 2001. New Mesozoic apparent polar wander path for south China: tectonic consequences, *J. geophys. Res.,* **106,** 8493–8520.

Yukutake, T. & Tachinaka, H., 1968. The non-dipole part of the earth's magnetic field, *Bull. Earthq. Res. Inst., Univ. Tokyo,* **46,** 1027–1074.

Zhou, X.M. & Li, W.X., 2000. Origin of Late Mesozoic igneous rocks in southeast China: implications for lithosphere subduction and underplating of mafic magmas, *Tectonophys.,* **326,** 269–287.

Zhu, B-Q., Wang, H-F., Chen, Y-W., Chang, X-Y., Hu, Y-G., & Xie, J., 2004. Geochronological and geochemical constraint on the Cenozoic extension of Cathaysian lithosphere and tectonic evolution of the border sea basins in East Asia. Jour, *Asian Earth Sci.,* **24,** 163–175.

Zijderveld, J.D.A., 1967. A.C. demagnetization of rocks: Analysis of results, in *Methods in Palaeomagnetism*, pp. 254–286, eds Collinson, D.W., Creer, K.M. & Runcorn S.K., Elsevier, Amsterdam.